Journal of Power Sources 249 (2014) 299–305

Contents lists available at ScienceDirect

Journal of Power Sources

journal homepage: www.elsevier.com/locate/jpowsour

Short communication

Corrosion resistance and electrical properties of carbon/chromium–titanium–nitride multilayer coatings on stainless steel

Kai Feng [a,b], Zhuguo Li [a,b,*], Fenggui Lu [a], Jian Huang [a], Xun Cai [a,b], Yixiong Wu [a,b]

[a] Shanghai Key Laboratory of Materials Laser Processing and Modification, School of Materials Science and Engineering, Shanghai Jiao Tong University, Shanghai 200240, China
[b] Academician Expert Office Workstation, Lin'an, Zhejiang Province, China

HIGHLIGHTS

- C/Cr–Ti–N multilayer coatings with varying Cr:Ti target current is deposited on SS316L.
- Metal ion corroded during 10 h potentiostatic test is reduced by more than 30 times by multilayer.
- Superior conductivity of around 2 and 3 mΩ cm^2 before and after 10 h polarization is achieved.

ARTICLE INFO

Article history:
Received 13 June 2013
Received in revised form
23 October 2013
Accepted 23 October 2013
Available online 4 November 2013

Keywords:
Physical vapor deposition
Multilayer
Bipolar plate
Interfacial contact resistance
Corrosion resistance
Fuel cell

ABSTRACT

High electrical conductivity and corrosion resistance are central to advances in wider application of metallic bipolar plates in polymer electrolyte membrane fuel cell (PEMFC). In this study, C/Cr–Ti–N multilayer coatings are deposited by physical vapor deposition and the effect of Cr:Ti ratio on the corrosion resistance and interfacial contact resistance (ICR) are systematically investigated. Scanning electron microscopy (SEM) result shows that the carbon layer is compact and uniform. Excellent corrosion resistance of 0.127 μA cm^{-2} current density at operating voltage in PEMFC cathode environment and low ICR of 2.03 mΩ-cm^2 at compaction force of 150 N cm^{-2} are achieved when Cr:Ti ratio is 2:4 and 3:3, respectively. The significant enhancement in surface conductivity is probably because that the current comes from carbon paper is homogenized by two electrically conductive layers and flows to the passive film with much more contact area. After polarization, ICR increase to 3.07 mΩ-cm^2 and 3.02 mΩ-cm^2 in the simulated PEMFC cathode and anode environment, respectively. However, the Raman spectroscopy results disclose that the bonding type of top carbon film before and after polarization shows little difference. The results indicate that C/Cr–Ti–N multilayer coating with Cr:Ti ratio of 2:4 achieves the optimal composition.

1. Introduction

The bipolar plate is a key multifunctional component in polymer electrolyte membrane fuel cell (PEMFC), which serves to separate individual cells, act as backbone of fuel cell stack, distribute the reactive gases uniformly, collect the electrical current, and remove the heat and water etc. [1,2]. Conventionally, graphite bipolar plate is widely used in PEMFC because of its high electrical conductivity and good corrosion resistance [3]. However, it is neither suitable for transportation applications that demand good structural durability against shock and vibration nor for large-scale manufacturing due to its poor mechanical strength. Currently, the dominating bipolar plate materials can be divided into composites and metals. Stainless steels are considered as one of the promising candidates because they permit properties such as high strength, ease of machining and shaping into thin sheets, low gas permeability and low cost [4,5]. Nevertheless, insufficient surface conductivity and corrosion resistance are two major drawbacks that prevent stainless steel from widely applied as bipolar plate material. Wang et al. [4] studied the electrochemical behavior of stainless steel 316L (SS316L), 317L, and 349TM in 1 M H_2SO_4 with 2 ppm F^- and the potentiodynamic test results showed that the current density of SS316L was as high as 10 μA cm^{-2}, which was one order of magnitude higher than the conventionally acceptable corrosion resistance for metallic bipolar plates as defined by the US Department of Energy (DOE) of ≤1 μA cm^{-2} [6]. Scholta [7] studied SS 316, 316L, and 316Ti in 1 M H_2SO_4 solution and noticed a current

* Corresponding author. Shanghai Key Laboratory of Materials Laser Processing and Modification, School of Materials Science and Engineering, Shanghai Jiao Tong University, Shanghai 200240, China. Tel.: +86 21 54745878; fax: +86 21 34203024.
E-mail address: lizg@sjtu.edu.cn (Z. Li).

0378-7753/$ – see front matter
http://dx.doi.org/10.1016/j.jpowsour.2013.10.103

density, as high as 3 mA cm^{-2} at 0.9 V_{RHE}. Wind et al. [8] also found a high dissolution rate of 316L in the single cell test. Kumagai et al. [9] barely observed corrosion on the anode side of SS304L but discovered substantial corrosion on the cathode side after operation for 1000 h. Therefore, for long term operation and duration concerns, surface modifications are still required in order to improve the surface conductivity and inhibit corrosion during service life of stainless steel bipolar plate in PEMFC [10,11].

Various coatings materials are normally divided into two categories by composition: carbon-based and metal-based [12,13]. Recently, carbon film has attracted extensive attentions because it combines the advantages of graphite and stainless steel with high electrical conductivity and chemical inertness [14,15]. Show et al. [14,16] prepared amorphous carbon film on titanium bipolar plates by chemical vapor deposition technique and their results showed that the fuel cell assembled with the a-C coated Ti bipolar plate has an output power of 1.4 times higher than that of bare Ti bipolar plate fuel cell. Fukutsuka et al. [15] deposited carbon coating on stainless steel 304 by plasma-assisted chemical vapor deposition. The carbon coated SS304 exhibited high electrical conductivity and improved corrosion resistance in spite of the absence of a passive film. Mori et al. [17] deposited a conductive amorphous carbon film on SS316L bipolar plates using electron cyclotron resonance plasma sputtering technique. This carbon film, mainly composed of sp^2 and sp^3 bonding, reduced the contact resistivity between the coated SS316L and carbon paper by two orders of magnitude. Fu et al. [18] prepared a C–Cr composite film on stainless steel by pulsed bias arc ion plating. The results showed that the interfacial conductivity and corrosion resistance were improved by the C–Cr film. In our previous research, amorphous carbon film with high percentage of sp^2 bond has been deposited on stainless steel by using closed field unbalanced magnetron sputtering ion plating (CFUBMSIP) [19–22]. This coating has good corrosion resistance and excellent surface conductivity that is even better than graphite due to the relatively large sp^2 component. With the optimization of deposition parameter, the interfacial contact resistance (ICR) of carbon film coated SS304 is minimized to 4.94 mΩ cm^2 at a compaction force of 135 N cm^{-2}, and the current density at 0.6 V in simulated PEMFC cathode environment is reduced to 2.10 μA cm^{-2} [22]. Yi et al. [23] tested this carbon film coated SS304 bipolar plate and in-situ experiments showed that the peak power density of the single cell using carbon film coated SS304 bipolar plates was twice of that using bare bipolar plates and the performance degradation after 200 h of continuous operation decreased from 28.7% to 3.9%.

However, due to the defects in the coating such as pinholes and macroparticles generated during PVD process, single layer coatings are usually prone to local corrosion and the current density has been reported to increase dramatically after long time immersion in the simulated PEMFC environment [24,25]. Recently, multilayer coatings have been shown to have improved performance over single layer coatings due to a reduced proportion of pinholes caused by the interruption of through-thickness pinholes [10,26,27]. Therefore, we fabricated a new multilayer coating composed of amorphous carbon as the outer layer and CrN as the inner layer (C/CrN multilayer) [28]. The results showed that the current density of C/CrN multilayer coated SS316L at 0.6 V is decreased to 0.5 μA cm^{-2} and ICR is minimized to 2.6 mΩ cm^2 at compaction force of 150 N cm^{-2} [28]. In this work, chromium target and titanium target are sputtered with different current to fabricated Cr–Ti–N ternary sub-layer with carbon coating on the top (hereafter nominated C/Cr–Ti–N multilayer coatings). It is expected to optimize composition and refine microstructure of sublayer, and subsequently to further improve corrosion resistance and surface conductivity of multilayer coating. The cross-sectional SEM, EDS line scan and bonding type of C/Cr–Ti–N multilayer coatings are studied by scanning electron microscopy (SEM) and dispersive Raman microscope. The electrochemical behavior and ICR are also systematically investigated and discussed.

2. Experimental details

2.1. Substrate materials and coating deposition

Austenitic stainless steel 316L purchased from Trinity Brand Industries, Inc. was used as substrate materials. The chemical composition was shown in Table 1. CFUBMSIP coating system (UDP 650, Teer Coatings, Ltd.) equipped with one chromium target, one titanium target and two graphite targets was used to deposit C/Cr–Ti–N multilayer coatings. After the chamber was depressurized at 3.0×10^{-5} torr, Ar was introduced into the chamber. Meanwhile, bias voltage of −500 V was applied to the substrate and 0.5 A chromium target current was used for 30 min to obtain a clean and active surface by sputtering. A thin Cr metallic seed layer was deposited when 6 A was supplied to Cr target to enhance adhesion. Afterward, a Cr–Ti–N, or CrN, or TiN layer was reactively sputtered in a mixture of argon and nitrogen and the flow rates were controlled to yield the required coating stoichiometry. In this process, the Cr:Ti target current ratio was keep at 6:0, 5:1, 4:2, 3:3, 2:4, 1:5 and 0:6 (hereafter nominated as C/CrN, C/Cr5Ti1N, C/Cr4Ti2N, C/Cr3Ti3N, C/Cr2Ti4N, C/Cr1Ti5N and C/TiN), respectively. Before deposition of the carbon coating, a thin intermediate MC_x layer (M: Cr or Ti) was deposited as an interfacial layer by reducing the current supplied to the chromium or titanium targets, and increasing simultaneously the current supplied to the carbon targets from 0.5 A to 5 A. Finally, the carbon layers were deposited outside. The detail deposition parameters were shown in Table 2.

2.2. Coating characterization

The surface morphology and cross section of the C/Cr–Ti–N multilayer coatings were observed by field-emission scanning electron microscopy (FE-SEM) of HITACHI S-4800. Energy-dispersive X-ray spectroscopy (EDS) was conducted to determine the cross section chemical distribution. In order to explore the change of bonding type and internal structure of carbon coating before and after the potentiostatic test, the Raman spectroscopy of carbon coating on as-received and polarized C/Cr4Ti2N sample was measured by dispersive Raman microscope Senterra R200-L (Bruker Optics).

2.3. Performance test

The electrochemical tests, including potentiodynamic and potentiostatic, were conducted using a Zahner Zennium electrochemical workstation to evaluate the corrosion resistance of the bare and C/Cr–Ti–N multilayer coated SS316L. The electrochemical tests were conducted in 0.5 M H_2SO_4 + 2 ppm HF solution at 70 °C to simulate the aggressive PEMFC environment. The solution was purged with either air (to simulate cathode environment) or hydrogen gas (to simulate anode environment) prior to and during the electrochemical test. A three-electrode system, in which the counter electrode was a platinum sheet, the reference electrode was mercury sulfate electrode (MSE), the working electrode was sample, was employed in this study. MSE, which was suitable for

Table 1
Chemical composition of SS316L (at.%).

Cr	Ni	Mo	C	Mn	Si	P	S	Fe
20.0–21.0	6.0–7.0	1.5	0.03	1.5	1.0	0.04	0.03	Balance

Table 2
Detailed deposition parameters of CFUBMSIP.

Process	Cr target current (A)	Ti target current (A)	C target current (A)	Bias voltage (V)	N_2 gas flow rate (SCCM)	Ar gas flow rate (SCCM)	Time (s)
Cleansing	0.5	–	–	−500	–	20	1800
Cr layer	0.5↗6	–	–	−500↘−60	–	−20	600
CrTiN	0–6	0–6	–	−60	0↗25	20	2700
MC_x	0–6↘0	0–6↘0	0.5↗5	−60	–	20	900
C layer	–	–	5	−60	–	−20	5400

sulfate solution, was separated from the solution by a Luggin capillary to avoid anion contamination. Before the electrochemical test, the open circuit potential (OCP) versus time was recorded for 1 h to ensure electrochemical stability. Potentiodynamic polarization was performed at a potential scanning rate of 1 mV s^{-1}. The potentiostatic test was carried out to investigate the performance and stability of the bare and C/Cr–Ti–N multilayer coated SS316L in the aggressive PEMFC environment. It was conducted for 10 h at a potential of 0.23 V vs MSE (equally to 0.6 V vs saturated calomel electrode (SCE)) while purging with air and −0.47 V vs MSE (equally to −0.1 V vs SCE) while purging with H_2 to simulate the cathode and anode operating environments, respectively. After the potentiostatic test, the solution was collected and analyzed by inductively-coupled plasma atomic emission spectrometry (ICP-AES) to determine the amounts of Fe, Cr, and Ni ions released into the solutions.

The ICR, which reflects through-plate conductivity between bipolar plates and gas diffusion layer, was measured by a sandwich structure. This structure consists of two pieces of conductive carbon paper (Toray TGP-H-090) sandwiched between the sample and two copper plates. A constant current of 0.1 A was applied through the two copper plates and the voltage drop was recorded when the compaction force was 150 N cm^{-2}. More details about the procedures can be found in the literature [4].

3. Results and discussion

3.1. SEM characterization

The surface morphology of the C/Cr–Ti–N multilayer coatings on SS316L is observed by SEM. Because similar surface morphology is observed for seven coatings due to the same carbon top layer on the surface, a typical surface morphology obtained from C/Cr4Ti2N sample is shown in Fig. 1(a). The carbon layer with spherical shape is compact and uniform and obvious pinhole is not observed within the observed area. The sound microstructure of C/Cr–Ti–N multilayer coatings results from high density of low energy bombarding ions surrounding the substrates and intense ion bombardment on the growing film during the deposition process. The cross-sectional SEM and EDS line scan of C/Cr4Ti2N sample is shown in Fig. 1(b). The result indicates that carbon is enriched in the top layer and Cr with little Ti is concentrated in the sub-layer. C/Cr–Ti–N multilayer coating shows a dense and non-column microstructure, which is expected to effectively inhibit corrosion of SS316L in PEMFC environment.

3.2. Electrochemical and ICP-AES tests

One of the most importance criterions in bipolar plate's performance is the corrosion resistance in fuel cell environment. The potentiodynamic polarization behaviors of the bare and C/Cr–Ti–N multilayer coated SS316L in 0.5 M H_2SO_4 + 2 ppm HF are shown in Fig. 2(a) and (b). Comparing polarization behavior of all samples,

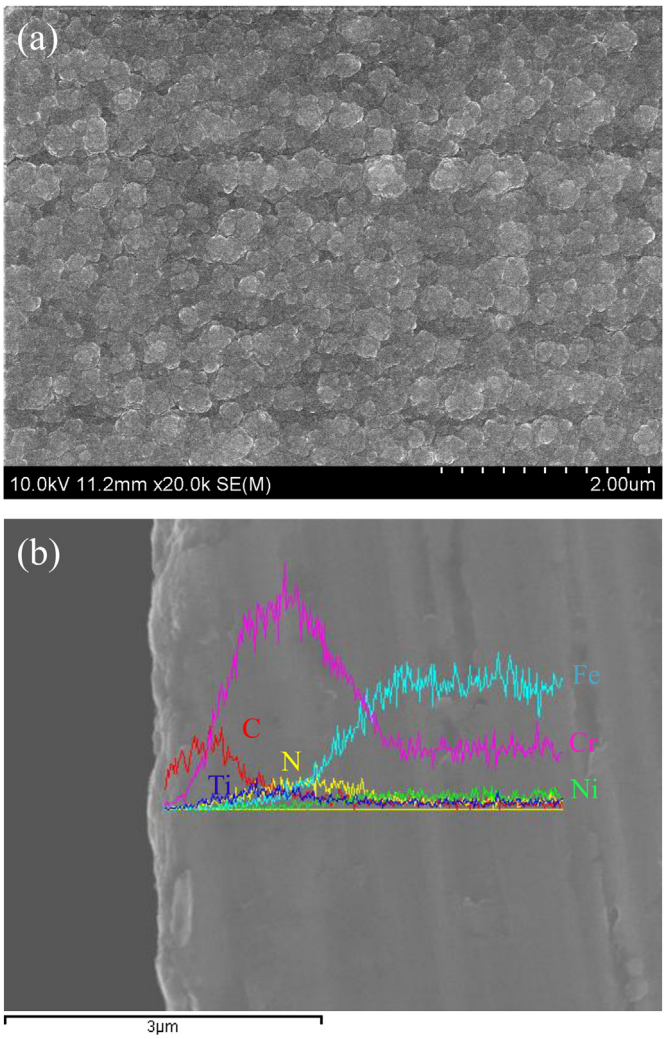

Fig. 1. SEM images of the typical surface morphology of C/Cr–Ti–N multilayer coating (a) and cross section and EDS line-scan of C/Cr2Ti4N samples.

the polarization curves of multilayer coated samples are quite different from that of the bare SS316L. Although bare SS316L exhibits a stable and wide passive region, the corrosion potential is more negative (−0.68 V vs MSE), indicating that it is more prone to corrosion. Moreover, the anodic working potential (−0.47 V vs MSE) is at the margin of the active region of the SS316L, which indicates SS316L may undergo unstable passivation in the anode environment. For multilayer coated SS316L, all of them show much nobler corrosion potential than bare SS316L and even anode working potential, reaching about −0.12 to −0.08 V vs MSE. Perspective from thermodynamics, a higher corrosion potential means higher chemical inertness and better corrosion resistance. Thus, C/Cr–Ti–N multilayer coated SS316L may be cathodically protected in simulated PEMFC anode environment. Fig. 2(b) displays the potentiodynamic polarization behaviors of the bare and C/Cr–Ti–N multilayer coated SS316L in simulated PEMFC cathode environment. Although SS316L exhibits a broader passive region ranging from −0.1 V to 0.9 V, the passivation current density at the cathodic operation potential (0.23 V vs MSE) is still as high as 11.26 μA cm^{-2}, which is unacceptable for bipolar plate materials. As for C/Cr–Ti–N multilayer coated SS316L, the passive region is much narrower compared to that of bare SS316L, which has adverse effect on stability in simulated PEMFC environment. However, due to the high chemical inertness of carbon coating, the corrosion potential

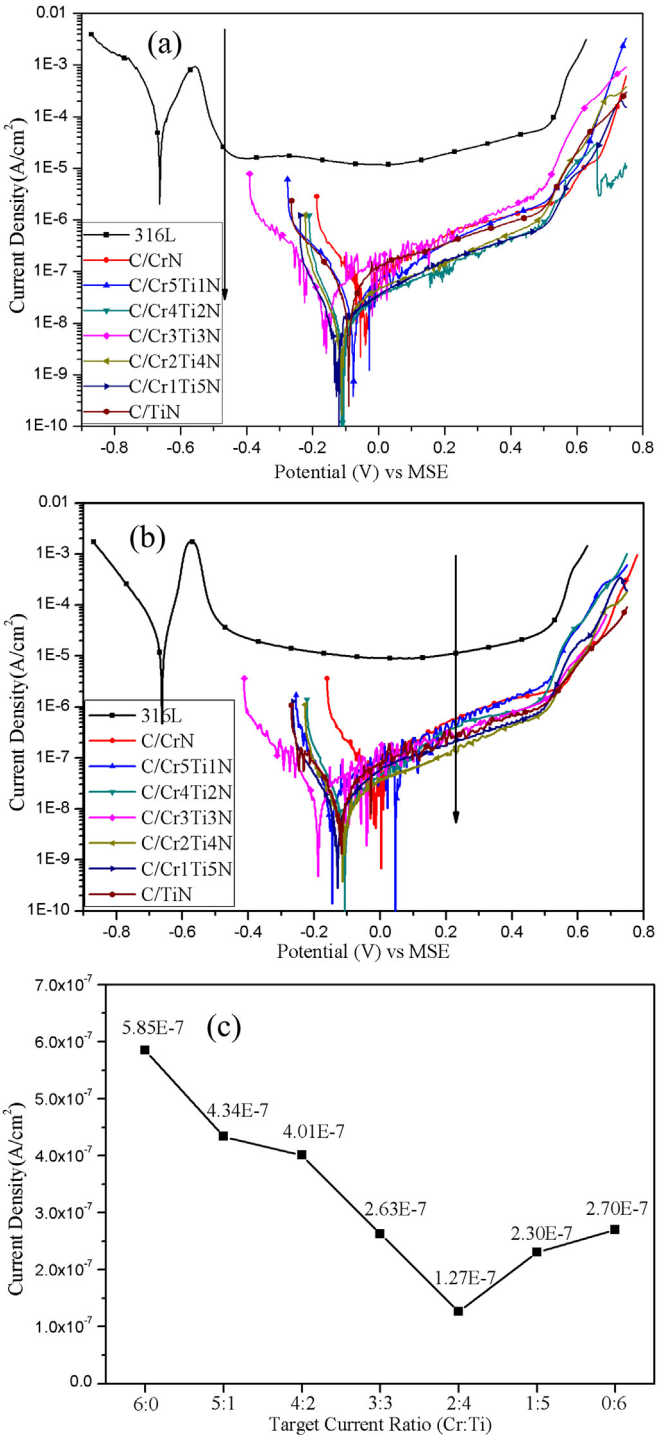

Fig. 2. Potentiodynamic curves of the bare and C/Cr–Ti–N multilayer coated SS316L in the simulated PEMFC environment: (a) bubbled with H_2 (anode environment) and (b) bubbled with air (cathode environment), and (c) current density versus Cr:Ti target current at cathodic working potential (0.23 V vs MSE).

of C/Cr–Ti–N multilayer coated SS316L shifts toward to the positive direction, reaching between −0.2 and 0 V vs MSE. The nobler corrosion potential significantly compromises the disadvantage of narrower passive region, and thus the current density of C/Cr–Ti–N multilayer coated sample at PEMFC cathode working potential is greatly decreased. Fig. 2(c) shows the variation of current density of C/Cr–Ti–N multilayer coated SS316L at PEMFC cathode operating potential versus Cr:Ti target current. Compared to the bare SS316L, the current density of C/Cr–Ti–N multilayer coated SS316L is much lower in value, in the range of 0.127–0.585 μA cm^{-2}. In specific, the current density decreases with the increasing target current of Ti, reaching minimized value of 0.127 μA cm^{-2} at Cr:Ti target current ratio of 2:4. Then the current density increases with the increasing target current of Ti, being 0.23 μA cm^{-2} and 0.27 μA cm^{-2}, for C/Cr1Ti5N and C/TiN sample, respectively. The potentiodynamic test results indicate that C/Cr–Ti–N multilayer coatings provide higher chemical inertness and better corrosion resistance in both the cathode and anode environments.

Potentiostatic test is conducted to benchmark the corrosion resistance of C/Cr–Ti–N multilayer coated SS316L at an applied potential (cathode 0.23 V vs MSE; anode −0.47 V vs MSE) in the simulated PEMFC environment. The current density at external applied potential as a function of operating time is recorded and presented in Fig. 3. Fig. 3(a) displays the potentiostatic curves at −0.47 V vs MSE in the anode environment. The current density obtained from the bare SS316L decreases with a positive current in the beginning because the applied potential of −0.47 V vs MSE is nobler than that of the bare SS316L. After that the current density gradually stabilizes to a low negative current indicating a stable passive film with a different composition is formed on the entire surface. Whereas the current density of C/Cr–Ti–N multilayer coated SS316L exhibits a different polarization behavior. It increases from negative direction in the beginning and gradually stabilizes at a lower current density due to nobler corrosion potential of C/Cr–Ti–N multilayer. The cathodic current discloses that the samples are cathodically protected because the corrosion potential of these samples is nobler than the anodic operation potential. As for the cathode environment presented in Fig. 3(b), the current density of the bare SS316L decreases gradually and then stabilizes at around 1.3 μA cm^{-2}, which is higher than the US DOE target of 1 μA cm^{-2}. While for all the multilayer coated SS316L samples, the stabilized current density is much lower than that of the bare SS316L, which disclose that less electrochemical reaction occurs on the interface between the carbon coating surface and adjacent electrolyte as well as lower metal ion release rates. The average current density at the end of potentiostatic test versus Cr:Ti target current is shown in Fig. 3(c). In specific, C/CrN and C/TiN multilayer coated SS316L exhibit the highest current density among these seven samples, being 81.5 nA cm^{-2} and 81.9 nA cm^{-2}, respectively. For C/Cr–Ti–N multilayer coated samples, the current density decreases with the increasing Ti target current in lower Ti target current region. Agreed well with the potentiodynamic test results, C/Cr–Ti–N multilayer coated SS316L achieves the minimized value of 24.2 nA cm^{-2}, which is more than two orders of magnitude lower than that of the bare SS316L.

After 10 h potentiostatic test, the metal ions in the solution released during corrosion are analysis by ICP-AES and the results are listed in Table 3. In general, all samples exhibit Fe ion selective dissolution due to its higher mobility in the passive film [29]. Metal ion concentration of the bare SS316L is much higher than that of C/Cr–Ti–N multilayer coated SS316L, being 9.19 ppm and 7.79 ppm in the simulated PEMFC cathode and anode environments, respectively. In contrast, the metal ion concentrations released from C/Cr–Ti–N multilayer coated SS316L are greatly reduced due to the higher chemical inertness and better corrosion resistance as indicated by electrochemical test results. Moreover, the metal ion concentration in anode environment is higher than that in the cathode environment. It is probably because hydrogen ion in anode environment is prone to penetrate into C/Cr–Ti–N multilayer coatings and cause active corrosion site leading to releasing of metal ions. Between the samples coated with multilayers, C/CrN and C/TiN samples show the highest metal ion concentration. In accordance with the electrochemical results, C/Cr2Ti4N sample has

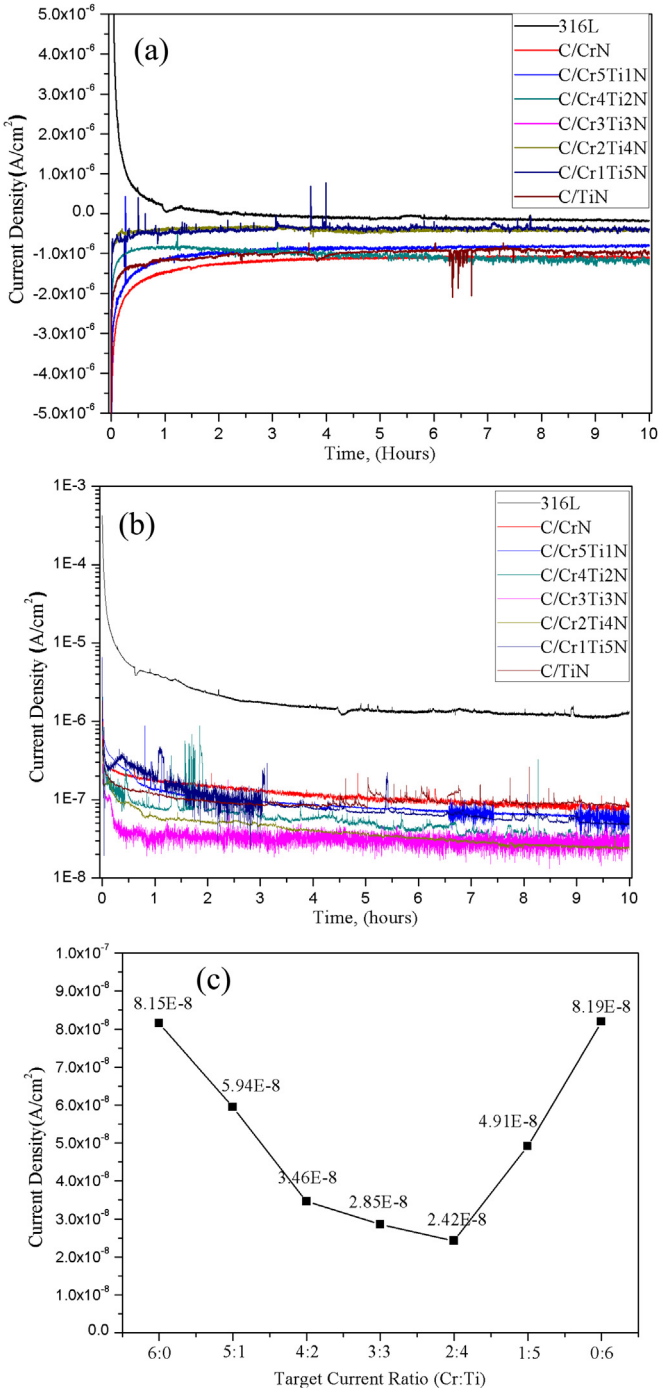

Fig. 3. Potentiostatic curves of the bare and C/Cr–Ti–N multilayer coated SS316L in the simulated (a) anode (−0.47 V vs MSE bubbled with H_2) and (b) cathode environment (0.23 V vs MSE bubbled with air), and (c) current density versus Cr:Ti target current at cathodic working potential (0.23 V vs MSE).

the lowest metal ion concentration, being 0.164 ppm and 0.211 ppm in the simulated PEMFC cathode and anode environment, respectively. Combining the electrochemical test results and ICP-AES result, it is demonstrated that C/Cr–Ti–N multilayer coatings with excellent corrosion resistance provide good protection for the stainless steel and even better than C/CrN and C/TiN multilayer coatings. Additionally, it is disclosed that the corrosion resistance of C/Cr–Ti–N multilayer is not only depending on the top carbon coating, but also relating to the chemical composition and microstructure of sub-layer materials.

3.3. ICR before and after polarization

Typically, the ICR decreases logarithmically with the compaction forces, which drops dramatically under lower compaction force while keeps a relative stable value at higher compaction force. In order to compare the ICR value at typical compaction force, the ICR values of C/Cr–Ti–N multilayer coated SS316L with different Cr:Ti target current are measured at a constant compaction force of 150 N cm^{-2}, respectively, with the bare, C/CrN and C/TiN multilayer coated SS316L as the references (shown in Fig. 4(a)). The bare SS316L exhibits an extremely high ICR value of 369.4 mΩ cm^2 because the semiconductor-like passive film produces a high electrical resistivity [30]. In contrast, the ICR of multilayer coated SS316L is quite low due to excellent electrical conductivity of carbon coating as well as sub-layer coatings. The ICR values of C/CrN and C/TiN multilayer coated SS316L are 2.67 and 2.97 mΩ cm^2, respectively. For C/Cr–Ti–N multilayer coated samples, the ICR value changes slightly with Ti target current in the order of C/Cr3Ti3N < C/Cr4Ti2N < C/Cr2Ti4N < C/Cr1Ti5N < C/Cr5Ti1N, which is lower than that of C/CrN and C/TiN multilayer coated samples. It can be seen that C/Cr3Ti3N sample achieves the lowest ICR value of 2.03 mΩ cm^2, which is much lower than the DOE 2020 technical target of ≤10 mΩ cm^2. In PEMFC working environment, the C/Cr–Ti–N multilayer undergoes polarization and corrosion, thus leading to change in composition, microstructure and ICR. Therefore, the ICR of multilayer coated SS316L after potentiostatic test is measured to investigate the effect of polarization on the surface conductivity of C/Cr–Ti–N multilayer coatings (shown in Fig. 4(b)). It is observed that the ICR of all C/Cr–Ti–N multilayer coated SS316L increase to 3.0–3.5 mΩ cm^2 after polarization. However, it still can satisfy the DOE 2020 technical target.

In this study, the ICR of C/Cr–Ti–N multilayer coated SS316L is remarkable lower than that of the bare SS316L. As compared to single layer coated stainless steel, the ICR of the C/Cr–Ti–N multilayer coated SS316L is still lower than that of TiN (30 mΩ cm^2 at typical compaction force [31]) and CrN (10 mΩ cm^2 at typical compaction force [32]), and is even lower than that of carbon coating of previous reported (6.8 mΩ cm^2 at compaction force of 150 N cm^{-2} [19,20]). The ICR is mainly influenced by both the contact area between the sample and carbon paper, as well as conductivity of the sample surface, which indeed affected by the composition and microstructure of surface materials. In this case, since the compaction force is identical and difference in surface morphology for all samples can be ignored compared to that of carbon paper, the remarkable reduction in ICR can be attributed to C/Cr–Ti–N multilayer coating. In order to illustrate the mechanism of reduction in ICR by multilayer coatings, the schematic diagram of current path between the carbon paper and different samples is shown in Fig. 5. It is known that stainless steel is usually encapsulated by a passive film with high electrical resistivity due to self-passivating. The surface of the bare and coated SS316L can be considered flat whereas the surface morphology of carbon paper is rather rough. As shown in Fig. 5(a), for the bare SS316L, the contact between the carbon paper and the passive film on SS316L is typical point contact. Therefore, the area of electrical conductive path through the passivation layer is small [17]. Moreover, passive film on stainless steel, which is composed of Fe oxides and Cr oxides, has very low electrical conductivity similar to semiconductor. Both of these two reasons lead to a high ICR value of the bare stainless steel. In the case of single layer coated stainless steel (shown in Fig. 5(b)), although the contact between the outside layer (TiN, CrN, carbon coating etc.) and carbon paper is still point contact, the contact between the outside layer and the passive film on stainless steel is plane contact. The current flow is probably homogenized and adjusted in the outside layer with good electrical conductivity.

Table 3
Fe, Cr, Ti, Ni ion concentrations corroded from the bare and C/Cr–Ti–N multilayer coated SS316L samples after 10 h potentiostatic test.

Sample	Ion concentration in PEMFC cathode environment after 10 h (ppm)					Ion concentration in PEMFC anode environment after 10 h (ppm)				
	Fe	Cr	Ti	Ni	Total	Fe	Cr	Ti	Ni	Total
S316L	7.62	0.88	–	0.69	9.19	6.28	0.90	–	0.61	7.79
C/CrN	0.614	0.025	–	0.025	0.664	0.651	0.015	–	–	0.666
C/Cr5Ti1N	0.447	0.019	0.003	0.014	0.483	0.499	0.011	0.006	0.002	0.518
C/Cr4Ti2N	0.194	0.009	0.004	0.015	0.222	0.387	0.012	0.008	–	0.407
C/Cr3Ti3N	0.268	0.006	0.017	0.005	0.296	0.311	0.003	0.008	0.001	0.323
C/Cr2Ti4N	0.148	0.004	0.012	–	0.164	0.195	0.011	0.005	–	0.211
C/Cr1Ti5N	0.373	0.005	0.021	0.004	0.403	0.406	0.008	0.015	0.002	0.431
C/TiN	0.581	0.002	0.023	0.018	0.624	0.603	0.006	0.022	0.004	0.635

Consequently, the current flow through the outside layer is parallel to the contact plane and the effective conductive path through the passive film is greatly enlarged [17]. In addition, the passive film between the single layer and stainless steel substrate is thinner than that on the surface of the bare stainless steel due to ion sputtering and cleansing before coating deposition. The above mentioned reasons make the ICR of single layer coated stainless steel greatly reduced compared to uncoated one. For multilayer coated stainless steel, the current is expected to be homogenized by two electrically conductive layers, including top layer (carbon coating) and sub-layer (Cr–Ti–N coating), thus flows more parallel to the passive film. This could be the reason why the ICR of C/Cr–Ti–N multilayer coated SS316L is lower than that of single carbon coated SS316L, even though they have the same chemical composition of top layer.

In this study, it is observed that the ICR of C/Cr–Ti–N multilayer coated SS316L slightly increases after the potentiostatic test. The carbon coating on the surface is not likely to change in the chemical composition, bonding type and density in the simulated PEMFC working environment, since the chemical inertness of carbon is similar to that of noble metal. In order to verify aforementioned assumption, we conduct Raman spectroscopy test to determine the detailed bonding structure in the carbon film before and after potentiostatic test. The results are shown in Fig. 6. No substantial difference is observed between the Raman spectra of as-received and polarized carbon coating, which indicates the same bonding type before and after polarization. On the other hand, noting that

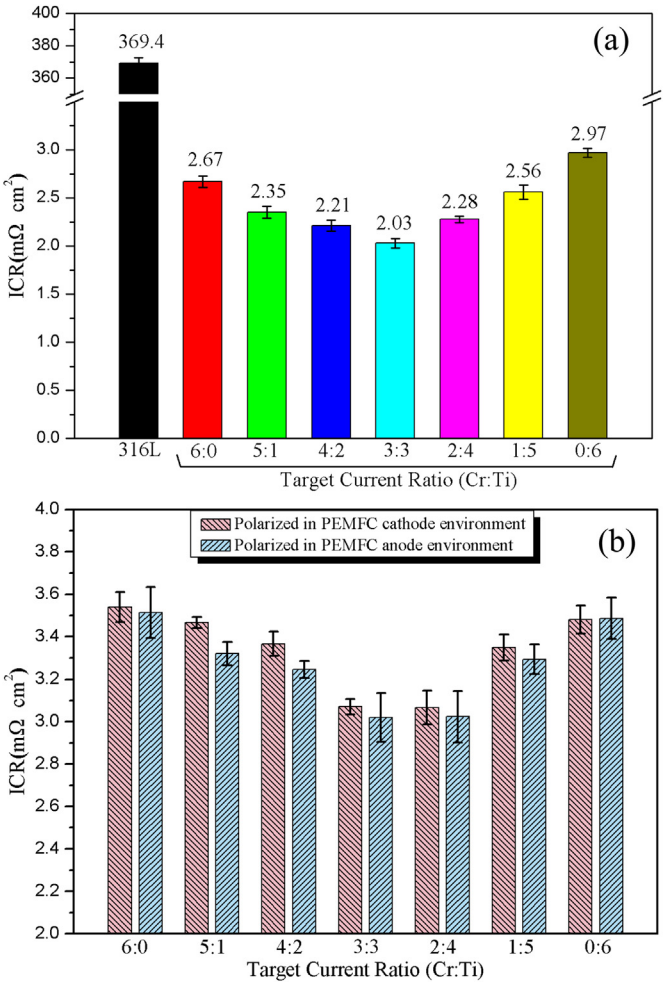

Fig. 4. (a) ICR values of C/Cr–Ti–N multilayer coated SS316L with different Cr:Ti target current with a constant compaction force of 150 N cm^{-2} (a) before and (b) after potentiostatic test in the simulated anode and cathode PEMFC environment.

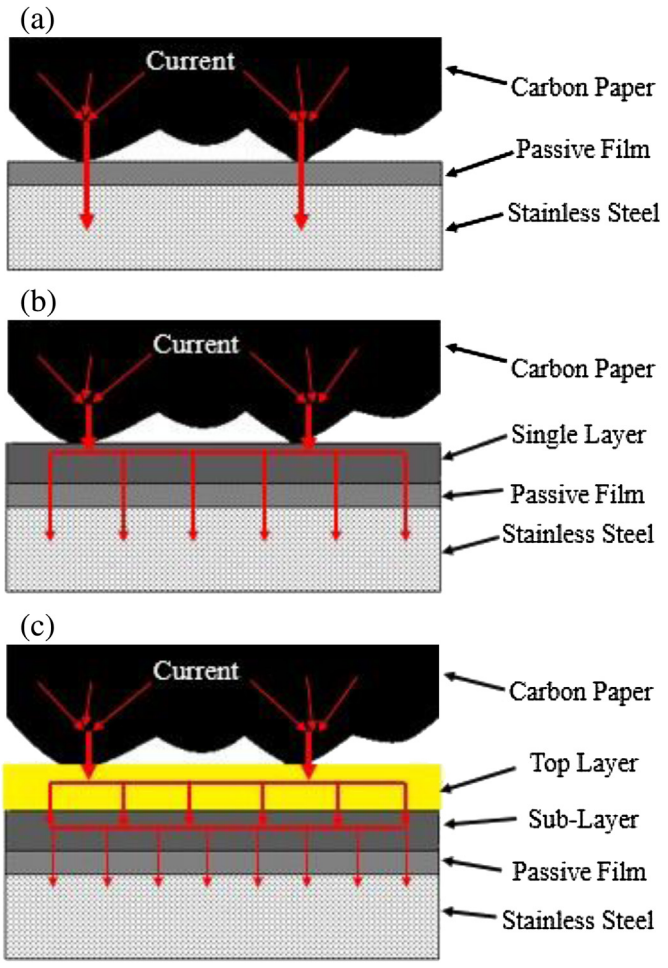

Fig. 5. Schematic diagram of current path between the carbon paper and (a) the bare stainless steel, (b) single layer coated stainless steel, and (c) multilayer coated stainless steel.

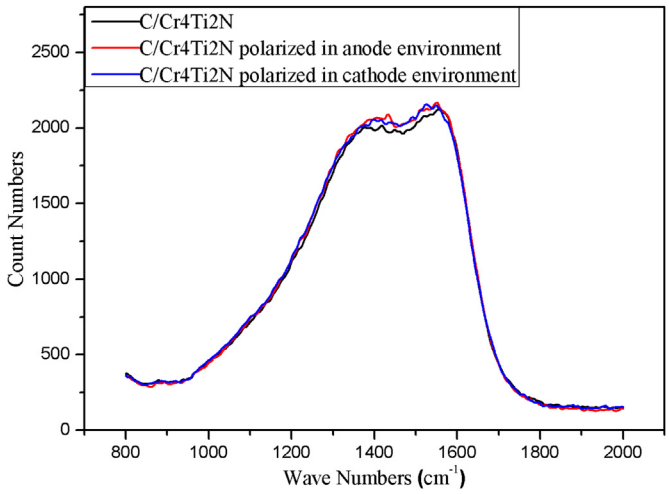

Fig. 6. Raman spectra obtained from: (a) as-received C/Cr4Ti2N; C/Cr4Ti2N sample after 10 h potentiostatic test in simulated PEMFC (b) anode and (c) cathode environment.

there is inevitable defect in the top carbon coating, the anion in the solution is prone to permeate though the carbon coating and react with Cr–Ti–N sub-layer. For most of these samples, the ICR of sample polarized in simulated PEMFC cathode environment is slightly higher than that of sample polarized in anode one. It can be well explained because Cr–Ti–N coating is more likely to be oxidized in the cathode environment, in which there is more anodic external applied potential and more oxygen.

In previous study, Yi et al. has tested the performance of fuel cell assembled with carbon coated stainless steel bipolar plates [23]. The results indicate that the peak power density of the single cell using carbon coated stainless steel bipolar plates is twice of that using the bare one. Furthermore, the performance degradation after 200 h of continuous operation decreases from 28.7% to 3.9%. Since the C/Cr–Ti–N multilayer coating provides better corrosion resistance and surface conductivity compared to the carbon coating investigated in previous study [19], we can expect a better assembled fuel cell performance using the C/Cr–Ti–N multilayer coating coated stainless steel bipolar plates.

4. Conclusions

C/Cr–Ti–N multilayer coatings are deposited on SS316L samples by CFUBMSIP technique and the effects of Cr:Ti target current ratio on the corrosion resistance and ICR are investigated experimentally. The SEM and EDS line scan of C/Cr4Ti2N sample show that the C/Cr–Ti–N multilayer coating is dense and uniform and with non-column microstructure. The potentiodynamic test results display that the corrosion potential of SS316L shifts significantly toward positive direction in both PEMFC anode and cathode environment, indicating much higher chemical inertness of C/Cr–Ti–N multilayer coating. The current density of C/Cr–Ti–N multilayer coated SS316L at cathodic operating potential of 0.23 V vs MSE in simulated PEMFC cathode environment is much lower than that of the bare one and C/Cr2Ti4N sample achieves lowest current density of 0.127 μA cm^{-2}. The potentiostatic and ICP-AES test results show that C/Cr–Ti–N multilayer coating provide effective protection against corrosion due to its dense structure and high chemical inertness. The total corroded ion concentration of C/Cr2Ti4N is lowest in all the samples, being 0.164 and 0.211 ppm in the simulated PEMFC cathode and anode environment, respectively. The ICR value of C/Cr–Ti–N multilayer coating changes marginally with Cr:Ti target current and achieving lowest value of 2.03 mΩ cm^2 for C/Cr3Ti3N sample. While after potentiostatic test, the ICR value of C/Cr3Ti3N and C/Cr2Ti4N become almost the same, being 3.07 mΩ cm^2 and 3.02 mΩ cm^2 in the simulated PEMFC cathode and anode environment, respectively. The superior surface conductivity of C/Cr–Ti–N multilayer coating is probably because that the current pass through is homogenized by two electrically conductive layers and flows more parallel to the passive film. Raman spectroscopy indicates that the bonding type of carbon coatings does not change after polarization. Our results reveal that the corrosion resistance and ICR are affected by both of top carbon coating and Cr–Ti–N sub-layer.

Acknowledgments

Financial support was provided by the National Natural Science Foundation of China under contract number 51201106, start-up fund for junior young teacher of Shanghai Jiao Tong University (Contract Number 13X100040022), and the Ministry of Science and Technology of the People's Republic of China (Grant No. 2009DFB50350).

References

[1] Y. Tang, W. Yuan, M.Q. Pan, Z.P. Wan, Int. J. Hydrogen Energy 35 (2010) 9661–9677.
[2] C.-H. Lee, Y.-B. Lee, K.-M. Kim, M.-G. Jeong, D.-S. Lim, Renew. Energy 54 (2013) 46–50.
[3] S.J. Lee, C.H. Huang, J.J. Lai, Y.P. Chen, J. Power Sources 131 (2004) 162–168.
[4] H. Wang, M.A. Sweikart, J.A. Turner, J. Power Sources 115 (2003) 243–251.
[5] A. Kumar, M. Ricketts, S. Hirano, J. Power Sources 195 (2010) 1401–1407.
[6] http://www1.eere.energy.gov/hydrogenandfuelcells/mypp/pdfs/fuel_cells.pdf 3.4-26.
[7] J. Scholta, B. Rohland, J. Garche, in: Proceedings of the 2nd International Symposium on New Materials for Fuel Cell and Modern Battery Systems, Ecole Polytechnique de Montreal, 1997, p. 330.
[8] J. Wind, R. Späh, W. Kaiser, G. Böhm, J. Power Sources 105 (2002) 256–260.
[9] M. Kumagai, S.T. Myung, S. Kuwata, R. Asaishi, H. Yashiro, Electrochim. Acta 53 (2008) 4205–4212.
[10] H. Sun, K. Cooke, G. Eitzinger, P. Hamilton, B. Pollet, Thin Solid Films 528 (2013) 199–204.
[11] R.A. Antunes, M.C.L. Oliveira, G. Ett, V. Ett, Int. J Hydrogen Energy 35 (2010) 3632–3647.
[12] H. Wang, J.A. Turner, Fuel Cells 10 (2010) 510–519.
[13] H. Tawfik, Y. Hung, D. Mahajan, J. Power Sources 163 (2007) 755–767.
[14] Y. Show, Surf. Coat. Technol. 202 (2007) 1252–1255.
[15] T. Fukutsuka, T. Yamaguchi, S. Miyano, Y. Matsuo, Y. Sugie, Z. Ogumi, J. Power Sources 174 (2007) 199–205.
[16] Y. Show, M. Miki, T. Nakamura, Diam. Relat. Mater. 16 (2007) 1159–1161.
[17] Y. Mori, M. Ueda, M. Hashimoto, Y. Aoi, S. Tanase, T. Sakai, Surf. Coat. Technol. 202 (2008) 4094–4101.
[18] Y. Fu, G. Lin, M. Hou, B. Wu, Z. Shao, B. Yi, Int J Hydrogen Energy 34 (2009) 405–409.
[19] K. Feng, Y. Shen, H. Sun, D. Liu, Q. An, X. Cai, P.K. Chu, Int. J. Hydrogen Energy 34 (2009) 6771–6777.
[20] K. Feng, X. Cai, H. Sun, Z. Li, P.K. Chu, Diam. Relat. Mater. 19 (2010) 1354–1361.
[21] W. Jin, K. Feng, Z. Li, X. Cai, L. Yu, D. Zhou, J. Power Sources 196 (2011) 10032–10037.
[22] W. Jin, K. Feng, Z. Li, X. Cai, L. Yu, D. Zhou, P.K. Chu, Thin Solid Films 531 (2013) 320–327.
[23] P.Y. Yi, L.F. Peng, L.Z. Feng, P. Gan, X.M. Lai, J Power Sources 195 (2010) 7061–7066.
[24] M. Li, S. Luo, C. Zeng, J. Shen, H. Lin, C. Cao, Corros. Sci. 46 (2004) 1369–1380.
[25] Y. Wang, D.O. Northwood, J. Power Sources 165 (2007) 293–298.
[26] H. Zhang, G. Lin, M. Hou, L. Hu, Z. Han, Y. Fu, Z. Shao, B. Yi, J. Power Sources 198 (2012) 176–181.
[27] R. Tian, J. Power Sources 196 (2011) 1258–1263.
[28] K. Feng, Z. Li, H. Sun, L. Yu, X. Cai, Y.X. Wu, P.K. Chu, J. Power Sources 222 (2013) 351–358.
[29] R. Kirchheim, B. Heine, H. Fischmeister, S. Hoffman, H. Knote, U. Stolz, Corros. Sci. 29 (1989) 899–917.
[30] A.K. Iversen, Corros. Sci. 48 (2006) 1036–1058.
[31] R. Tian, J. Sun, Int. J. Hydrogen Energy 36 (2011) 6788–6794.
[32] Y. Fu, M. Hou, G. Lin, J. Hou, Z. Shao, B. Yi, J. Power Sources 176 (2008) 282–286.